Basic walker-assisted gait characteristics derived from forces and moments exerted on the walker's handles: Results on normal subjects

Majd Alwan [a,*], Alexandre Ledoux [b], Glenn Wasson [c], Pradip Sheth [b], Cunjun Huang [b]

[a] *Medical Automation Research Center (MARC), P.O. Box 800403, Charlottesville, VA 22908, USA*
[b] *Department of Mechanical and Aerospace Engineering, University of Virginia, USA*
[c] *Computer Science Department, University of Virginia, USA*

Abstract

This paper describes a method that passively assesses basic walker-assisted gait characteristics using only force-moment measurements from the walker's handles. The passively derived gait characteristics of 22 subjects were validated against motion capture gait analysis. The force-moment based heel initial contact detection algorithm have produced a high level of concordance with heel initial contacts detected by a human inspecting the heel marker data sets of the Vicon video capture system. The algorithm has demonstrated 97% sensitivity and 98% specificity with a narrow 95% confidence interval of $\pm 1\%$ during all experiments, which included five navigational scenarios.

Temporal error in detecting the instances of heel initial contacts were within $5.27 \pm 3.66\%$ of the overall stride time obtained from Vicon when the subjects walked in a straight line, whereas the toe-off instance estimates were within $5.18 \pm 2.75\%$ of the gait cycle. The errors in determining the duration of stride time, single support, and double support were within $5.86 \pm 2.49\%$, $5.24 \pm 2.29\%$, and $4.34 \pm 2.13\%$ of the gait cycle respectively. The stride time estimated, using the method presented here, correlated well with stride time computations based on visual inspection of Vicon's data, Pearson correlation coefficient $r = 0.86$ for straight line segments. However, absolute errors were too high to estimate the single and double support phases with acceptable accuracy. The potential application of the instrumented walker and the method presented here is longitudinal basic gait assessment that can be performed outside of the conventional gait labs.
© 2006 IPEM. Published by Elsevier Ltd. All rights reserved.

Keywords: Walker-assisted gait; Passive assessment of gait characteristics; Detection of heel initial contact; Detection of gait phases

1. Introduction

Independent mobility is one of the most important factors in maintaining quality of life for elders, and other clinical populations who need assistive devices such as walkers. Mobility is crucial for performing the activities of daily living (ADLs), as well as maintaining fitness and vitality [1]. Reduced quality of life has been associated with factors indicative of reduced mobility such as the inability to ascend stairs, fatigue and social activity. Longitudinal assessment of functionality of mobility aid users, both inside and outside the home, can provide clinicians with continuous measures of a person's functional ability and activity levels. Moreover, functional assessment in the user's natural environment, i.e. outside the clinic and the gait lab, is useful for monitoring the effectiveness of therapeutic interventions including surgeries, pharmaceutical interventions, or physical therapy over extended periods of time.

Second only to the cane, walkers are used more often than any other mobility aid [2], however, walker-assisted gait has not been fully investigated. In several research projects walkers have been instrumented for control purposes, such as the inference of the intent of the walker's user to implement control [3]. However, few researchers have attempted to instrument a walker to assess the functionality of the walker-dependent user. One of these attempts is the work of Fast et al. [4] where strain gauges were mounted on all four legs of a walker to record forces transmitted through the walker's frame in axial, frontal and sagittal orientations.

* Corresponding author. Tel.: +1 434 924 2265.
E-mail address: ma5x@virginia.edu (M. Alwan).

The instrumented walker provided a better understanding of loading and force distribution in clinical populations including two primary modes of use for weight support and balance enhancement, as well as a combination of these two modes. In another study [5], a pick-up walker instrumented with strain gauges was developed to measure the six-axis resultant force-moments applied by the user and a finite-element model of the walker was developed to analyze the loading patterns [5]. Chen et al. [6] instrumented a cane to understand the underlying biomechanics of temporal stride and force in people with hemiplegic stroke during cane-assisted walking. The instrumented cane data could be useful in assessing the nature of cane assistance and in planning therapeutic strategies for people with stroke [6]. None of these studies explored the potential use of the measured force and moments to passively derive basic gait characteristics.

Finally, there is abundant literature on attempts to derive gait characteristics by instrumenting the subject using accelerometers and/or gyroscopes, primarily for the purpose of controlling functional electrical stimulators (FES) [7–11]; however, these methods rely on the user's compliance in wearing the device and are hence not passive.

This paper builds on previous research performed at the University of Virginia in using instrumented wheeled walkers to develop a human/machine shared-control system that assists users by increasing the safety and speed of their daily travel [3,12,13]. Here we present the use of a walker instrumented with force-moment sensors to passively derive basic gait characteristics. It is hypothesized that the forces and moments recorded from the walker's handles will have cyclic changes reflecting the gait cycle, and that from these changes basic gait characteristics such as step count, pace, and stride time and possibly gait phases including double support, as well as right and left single support could be correctly identified.

Wheeled walkers can be easily augmented with simple and relatively low-cost instrumentation technologies to provide a wide range of functionality and gait characteristics. Such a device would provide *in situ* gait analysis technology that may overcome the problems that plague routine clinical use of gait analysis such as the manner in which gait laboratories are organized, tests are performed, and reports are generated, as well as the length of time and costs required for performing tests and interpreting the results [14]. However, the device is not intended to be an alternative for gait analysis laboratories, whose aim is to perform a global and accurate evaluation of the different components of movement (kinematic, kinetic, EMG, etc.), but rather a tool for the longitudinal evaluation of basic temporal features of gait in the field.

2. Methodology

2.1. Walker and data acquisition systems

The walker is a standard Sprint® three-wheel rollator (Invacare, OH, USA), augmented with two 6-DoF load cells
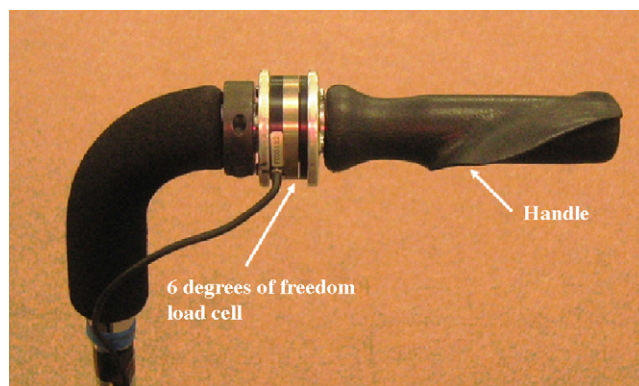

Fig. 1. The load cell for measurement of user forces and moments applied to the walker's handle.

US120-160 (ATI Industrial Automation, NC, USA). The walker's handles were sawn and the sensors were mounted in-line between the handles and the walker's frame, as shown in Fig. 1. The sensors provide the load/moment transfers between the walker and the user. The force-moment signals were sampled at 360 Hz using a laptop personal computer mounted on the walker and equipped with two PCMCIA data acquisition cards. The motion model (walker/user) was captured using reflective markers and the Vicon 612® motion analysis system (Vicon Motion Systems, Oxford, UK) connected to six 120 Hz video cameras [15]. The Vicon system and the force-moment data acquisition computer were synchronized using a synchronization channel between the two systems. The Vicon system can create a 3D motion model by using the positions in the (x–y–z) space of particular real points (markers) placed on the human and the walker frame. In this model, seven markers represented the walker and four were placed on the toes and heels of the participant. The Vicon motion capture system was chosen as a reference in the experiments, since the experiments also aimed at capturing the trajectory of the walker as well as the user's forces and moments in different scenarios in attempt to understand the User's Navigational Intent (see Ref. [3]). The global coordinate system of Vicon is aligned with the local coordinate system of the force-moment measurement system, which is tied to the walker's frame, at the beginning of every experiment. The vertical component of the trajectory of the heel (calcaneous) and toe (metatarsal) markers were used to determine the Vicon heel initial contact and toe-off instances.

A flat amplitude response IIR low-pass filter with a cut-off frequency of 3 Hz is used in filtering the force-moment data. To eliminate the phase shift caused by filtering, a non-causal bi-directional filter was implemented. This filter performs zero-phase shift digital filtering by processing the force-moment data in both the forward and reverse directions [16].

2.2. Subjects

Experiments were conducted in the gait lab on a total of 22 participants, 15 of whom were older adults (above 65). Sub-

jects had a mean age of 64.6 ± 15.2 years (minimum = 27, maximum = 87 years), a mean height of 169.1 ± 8.1 cm (minimum = 158, maximum = 183 cm), and a mean weight of 75.7 ± 9.2 kg (minimum = 59.4, maximum = 95.2 kg). None of the subjects depended on a walker or presented any locomotion disabilities. All subjects reviewed the experimental protocol approved by the Institutional Review Board (IRB) and signed an informed consent prior to participation.

2.3. Experimental procedure

Each user performed a total of 15 experiments emulating 5 navigational scenarios designed to determine navigational intent from measured forces and moments recorded at the handles of the walker; a pre-experiment trial was aimed at calibrating the data capture systems. The navigational scenarios included walking in a straight line, and turning right and left at two different angles on each side. Each navigational scenario was performed three times.

2.4. Observed force-moment patterns, and detection algorithms

Careful examination of all force-moment channels, expressed in the local coordinate system, against the right and left heel markers' data revealed a pattern indicating a correlation between the forces-moments in the direction normal to the ground, F_Z, the corresponding moment around the axis parallel to the ground and perpendicular to the direction of travel, M_X, and the vertical component of the trajectory of the heel markers. Peaks in F_Z and the corresponding moment M_X signals coincided with heel initial contact; heel initial contacts were identified as the valleys in the vertical component of the trajectory traces of the heel markers. However, the pattern was clearer in the moment signal due to the lever effect of the handles' length, so we chose to use the right and left M_X moment signals. Right and left M_X signals show two peaks, one with higher amplitude coinciding with heel initial contact of the corresponding foot, the other with lower amplitude coinciding with heel initial contact of the opposite foot; these higher and lower peaks alternate repetitively. This pattern reflects the lateral sway motion of the upper body of the walker's user during ambulation, which can be modeled as an inverted pendulum, and the associated pattern of loading exerted on the walker frame. The load is transmitted through the walker's rigid frame and could be measured by ground reaction forces. This pattern in the force-moment signals was exploited in developing a peak detection algorithm to identify right and left heel initial contacts from the right and left M_X signals. A simple off-line peak detection algorithm was sufficient to produce encouraging preliminary results; these were reported in Ref. [17]. Later, more sophisticated dual-step peak detection was implemented. The first step of the peak detection algorithm examines data from the right and left M_X signal to estimate the approximate time of each heel initial contact. This peak detection algorithm has produced better results when applied to the signal representing the summation of the right and left moment signals around the X-axis ($M_{X,\text{left}} + M_{X,\text{right}}$); this is due to the fact that peaks corresponding to heel initial contacts were enhanced because they were present in each one of the two added signals, unlike spurious peaks, which could be due to noise. The second step of the algorithm detects the actual timing of the heel initial contacts by analyzing the signal $M_{X,\text{left}}$ and $M_{X,\text{right}}$ independently. The estimated heel initial contact time, computed from first step, is exploited to create relatively narrow time windows centered at the estimated heel initial contact times. All trials from eight randomly selected subjects were used to determine the best size of the window; the optimization was based on selecting a window width that did not miss any heel initial contact and that minimized the error between the time of heel initial contacts detected by the peak detection algorithm and the heel initial contact times provided by human detection on Vicon's data. The results presented below are computed using only one size window for all subject. The single window size demonstrates the robustness over the subject population tested. Better results could be obtained if the algorithm utilized a user-specific window. The peak detection algorithm analyzes the signal in these windows, as shown in Fig. 2, to compute the accurate heel initial contact instances. The window method allows the identification of heel initial contacts more accurately (i.e. minimizes the absolute error between actual heel initial contacts and peaks identified in the moment signal), but it may result in missing some peaks in each signal. To determine whether the detected peak corresponded to the right or left heel initial contact, the original right and left M_X signals were examined as explained earlier.

The off-line peak detection algorithm described above was applied as a post-processing analysis to all trial data sets. The algorithm scans the M_X data recorded for the whole trial to find the highest peak. Once this peak is detected, the algorithm starts to iteratively search for the remaining peaks after skipping a portion of the data that reflects a pre-determined dead-time to avoid the detection of false peaks in the undulating M_X signal that do not coincide with heel initial contacts. The algorithm stops when the amplitude of the current peak in sum of moments ($M_{X,\text{left}} + M_{X,\text{right}}$) signal falls under a threshold of 1 Nm. This algorithm has demonstrated robustness on all our trial data sets. However, the algorithm is not suited for on-line processing.

Similarly, the data sets exhibited a pattern between the forward propulsion forces applied by the user, F_Y, and the toe-off event from the right and left toe markers' data captured by Vicon; toe-off events were identified as the start of a significant rise in the trajectory traces of the toe markers. For some users the toe-off events coincide with the start of an appreciable increase in the forward pushing force on the handle. Alternatively, the toe-off times can be estimated using a 60% rule based on the detected heel initial contact event. Two successive heel initial contacts, measured for the same foot, are used to compute the stride (i.e. the duration of the gait cycle). Using a normalized gait diagram [18], we can com-
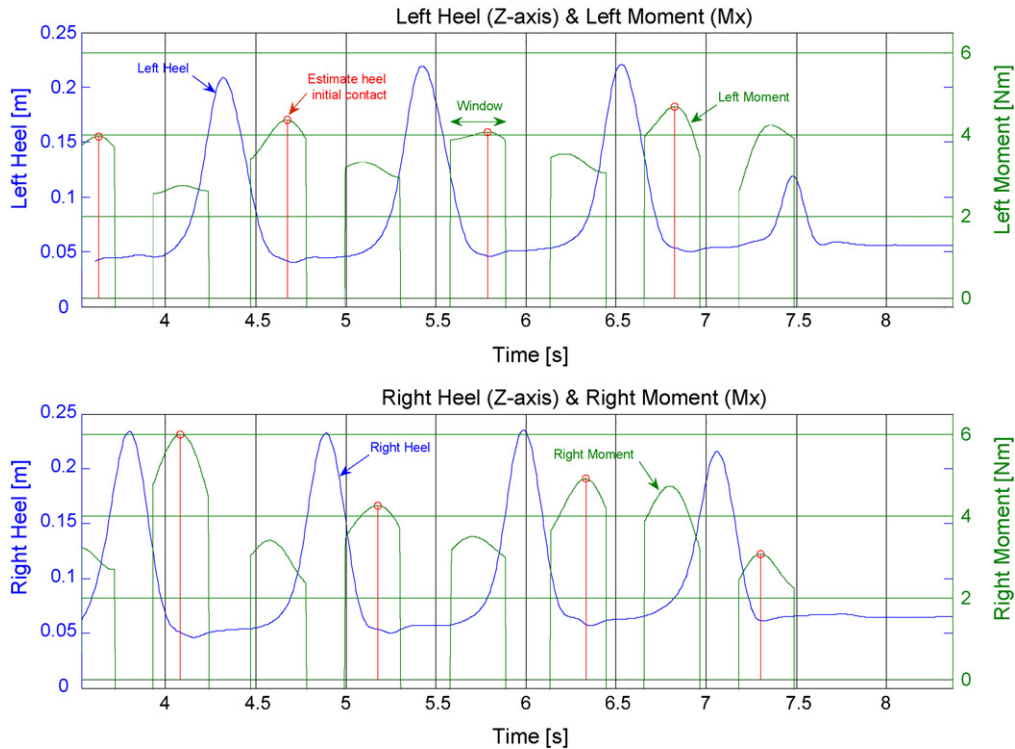
Fig. 2. Heel initial contact detection algorithm—left and right initial contacts are obtained in windows centered on estimated heel initial contact times. Peaks in the moment signal marked by circles coincide with valleys in the corresponding heel marker's vertical signal; vertical lines are drawn from these peaks to show relation to the heel initial contact instance.

pute an estimate of the toe-off event by adding 60% of the stride to the time of the first detected heel contact. Repeating the process, we can obtain an estimate of all the subsequent toe-off events.

2.5. Statistical methods

Two by two contingency table and the chi-square statistics were used to evaluate the concordance between the heel initial contact detection and the toe-off estimation algorithms, and heel initial contact and toe-off events detected by a human observer inspecting Vicon's motion data, respectively. Errors in the detection time between the algorithm and the Vicon based detection were computed for heel initial contact and toe-off events, stride time, as well as single and double support gait phases.

3. Results

3.1. Heel initial contact detection results

Fig. 3 shows typical graphs of the left (top) and right (bottom) heel marker data and the moment M_X exerted on the corresponding handle from one of the subjects. Notice how peaks in the moment signal, marked by circles, coincide with valleys in the corresponding heel marker signal; vertical lines are drawn from these peaks to show relation

to the heel initial contact instance. Similarly, peaks in the moment signal, marked by +, coincide with valleys in the opposite heel marker signal. The data set selected is trial no. 2 of subject no. 7, and it was selected to show the robustness of the peak detection method despite the small variations in the M_X moment compared to other trial data sets from the same subject, as well as data sets from other subjects.

Fig. 4 shows the worst case where the heel initial contact detection algorithm performed poorly. The data set presented is from subject no. 7 performing a sharp (60°) turn to the left. The algorithm missed the third heel initial contact of the left foot.

The accuracy of the heel initial contact detection algorithm was established on a step-by-step basis, through comparison to the count of steps detected by human observer inspecting the heel marker signals from the Vicon system, using two-by-two contingency table and the chi-square statistics. Data were considered as nominal. The two-by-two tables were constructed in the context of a detection algorithm as shown in Table 1. Heel initial contacts detected by the algorithm and observed on the Vicon heel marker signals within the same step time window was scored as a hit or a true positive. If the algorithm did not report an observed heel initial contact within Vicon's step time window, a miss or a false negative occurred. Heel initial contacts detected by the algorithm, but not observed on the Vicon data was scored as a false positive detection. Finally, if neither the algorithm nor the Vicon reported a heel initial contact, a true negative was recorded.
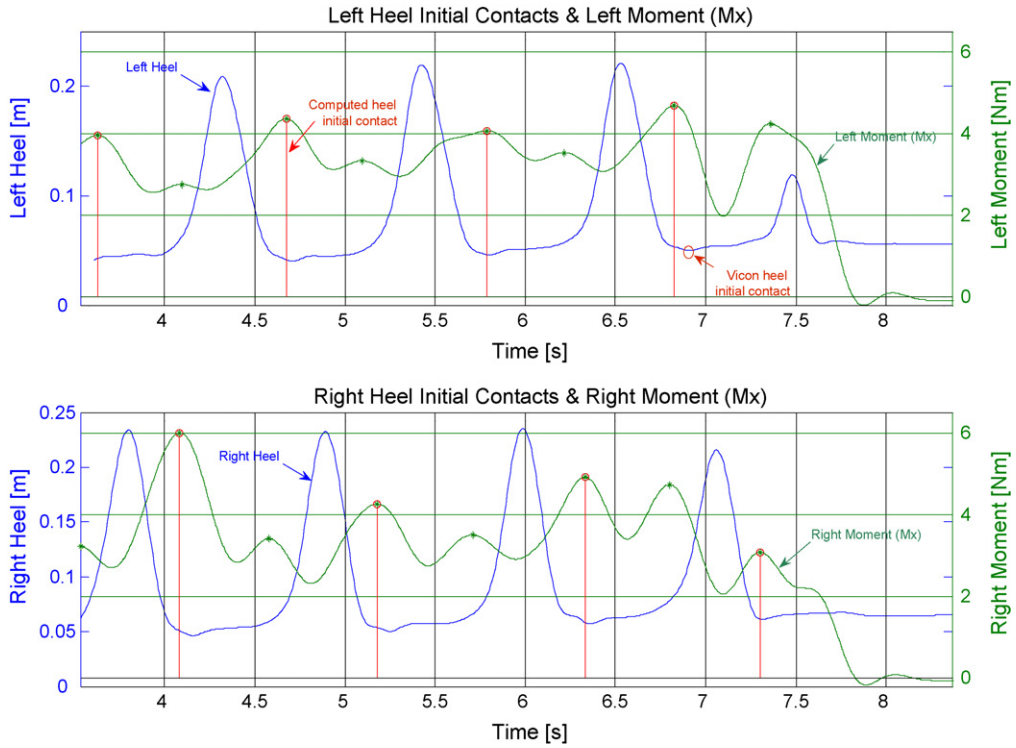
Fig. 3. Peaks in M_X signals coinciding with heel initial contacts (valleys) obtained from the heel marker's vertical signals. Peaks in the moment signal, marked by circles, coincide with valleys in the corresponding heel marker signal; vertical lines are drawn from these peaks to show relation to the heel initial contact instance. Similarly, peaks in the moment signal, marked by '+', coincide with valleys in the opposite heel marker signal.
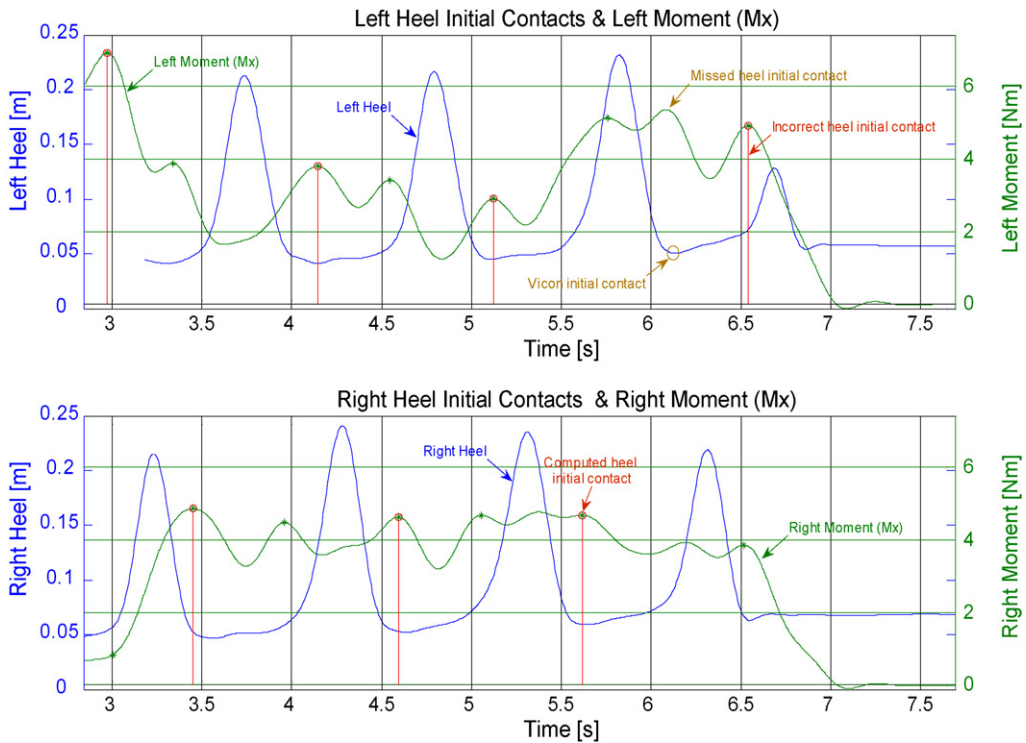

Fig. 4. Worst case performance of the heel initial contact detection algorithm—the third left heel initial contact (top) is missed.

Table 1
Two-by-two contingency table used in evaluating the accuracy of the detection algorithm

Vicon	Algorithm	
	Detected	Not detected
Heel initial contact	Hit (true positive)	Miss (false negative)
No heel initial contact	False detection (false positive)	True negative

Table 2
The *p*-value, sensitivity, and specificity of the heel initial contact detection algorithm on a step-by-step basis (together with their 95% confidence interval (CI)) obtained using the chi-square test

	p	Sensitivity (95% CI)	Specificity (95% CI)
Go straight	<0.0001	1 (0.99–1.00)	0.97 (0.95–0.99)
30° left turn	<0.0001	0.96 (0.93–0.98)	0.93 (0.89–0.96)
30° right turn	<0.0001	0.96 (0.93–0.98)	0.96 (0.93–0.98)
60° left turn	<0.0001	0.97 (0.95–0.99)	1 (0.99–1.00)
60° right turn	<0.0001	0.97 (0.95–0.98)	1 (0.99–1.00)
Overall	<0.0001	0.97 (0.96–0.98)	0.98 (0.97–0.98)

A total of 1577 steps from all trials of all subjects were analyzed and the results, summarized in Table 2, show that the algorithm has a high sensitivity and specificity. Sensitivity probabilistically measures the algorithm's ability to correctly detect an observed step, or true positives, where as specificity characterizes the algorithms ability to correctly identify true negatives. The algorithm detected the heels' initial contact with sensitivity ranging from 96% to 100% and specificity ranging from 93% to 100%; the results were statistically significant for all navigational scenarios tested.

Further, correlation coefficients and the errors between the heel initial contact instances obtained from visual inspection of Vicon data and those derived from moment data for all trials are presented in Table 3. Errors are presented both as an absolute difference and as a percentage of the duration of the overall gait cycle measured from Vicon's data. The minimum correlation coefficient for the heels' initial contact between our algorithm and the inspection of Vicon's data was 99.63%, while the maximum temporal error in the detection of these instances was 95.08 ± 79.46 ms.

3.2. Toe-off detection results

The toe-off detection algorithm did not perform as well as the heel initial contact detection algorithm on all the subjects. The algorithm did not have reproducible results on all data sets from all the subjects, and had large errors in the toe-off event detection. Subject no. 7 in particular challenged the toe-off detection algorithm possibly due to lower changes in the forces exerted by this individual. A more sophisticated algorithm may allow the detection of these instances even with small force and moment variations. However, in the current implementation of the algorithm, better results were obtained using the toe-off estimation method presented in the methodology section.

Table 3
Pearson correlation coefficients (*r*) and mean of the absolute errors in heel initial contact detection between Vicon based inspection and the force-moment based algorithm (presented as absolute time difference, in milliseconds, between the instances of initial contact identified on Vicon and the corresponding initial contacts detected by our algorithm, as well as the percentage of this time difference to the corresponding stride time obtained from Vicon)

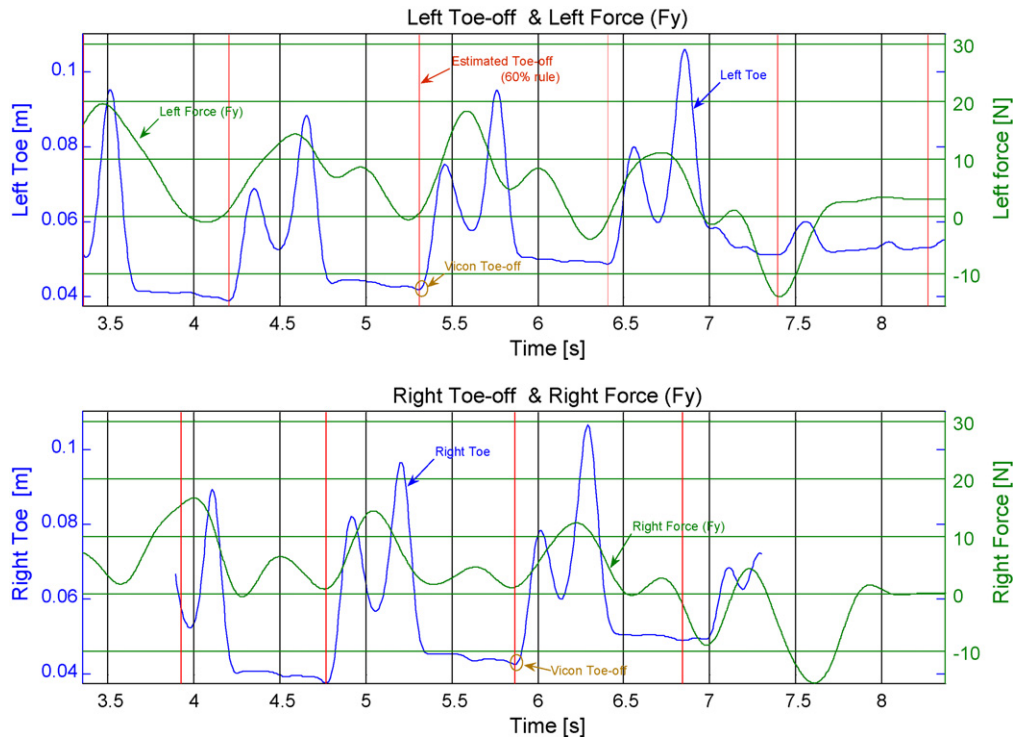|	Go straight	30° left turn	30° right turn	60° left turn	60° right turn
Right heel	0.9990, 5.27 ± 3.66% (67.26 ± 50.38 ms)	0.9985, 5.78 ± 3.16% (72.72 ± 44.29 ms)	0.9963, 6.19 ± 5.48% (70.14 ± 44.06 ms)	0.9981, 6.46 ± 5.73% (84.44 ± 80.29 ms)	0.9984 5.63 ± 3.33% (70.80 ± 40.54 ms)
Left heel	0.9987, 5.05 ± 2.78% (63.97 ± 37.05 ms)	0.9988, 5.71 ± 4.08% (69.70 ± 51.01 ms)	0.9968, 5.46 ± 6.92% (57.75 ± 52.01 ms)	0.9973, 7.27 ± 5.43% (95.08 ± 79.46 ms)	0.9977 7.12 ± 3.66% (89.20 ± 48.37 ms)

Fig. 5. Toe-off instances vs. the toe-off estimate based on the 60% of stride time rule.

3.3. Toe-off estimation results

As an alternative to the toe-off detection algorithm, the toe-off times were estimated using a 60% rule based on the detected heel initial contact event. Fig. 5 graphically presents the results of toe-off estimation using the 60% estimation rule mentioned above.

Table 4 summarizes the errors between the toe-off instances obtained from visual inspection of Vicon data and those estimated using the 60% rule for all trials. Errors are presented both as an absolute value and as a percentage of the duration of the overall gait cycle measured from Vicon's data. The minimum correlation coefficient for the toe-off between the 60% estimation rule and the inspection of Vicon's data was 99.59%, while the maximum temporal error in the detection of these instances was 103.56 ± 83.73 ms.

3.4. Gait cycle, double support, and right and left single support results

Finally, we computed the stride time, double support, as well as the right and left single support phases based on our heel initial contact detection algorithm and our toe-off estimation rule, and compared the results to those obtained from the heel initial contact and toe-off instances obtained directly from visual inspection of Vicon's data. Correlation coefficients between the two methods, percent errors, relative to the duration of the overall gait cycle measured from Vicon's data, as well as the absolute errors in milliseconds, are tabulated in Table 5. The minimum correlation coefficient between

gait phases derived from the force-moment data compared to Vicon's motion capture data was that for the double support time, 17.12%, while the maximum temporal error was for the stride time during sharp turns 110.61 ± 69.43 ms.

4. Discussion

4.1. Errors and their possible sources

The heel initial contact detection algorithm from force-moment data have produced a high level of concordance with heel initial contacts detected by a human inspecting the heel marker data sets of the Vicon video capture system. The algorithm has demonstrated 97% sensitivity and 98% specificity with a narrow 95% confidence interval of ±1% during all experiments, which included five navigational scenarios. Temporal error in detecting the instances of heel initial contacts was within 74.74 ± 54.88 ms, which is equivalent to $6.19 \pm 4.91\%$ of the overall stride time obtained from Vicon, whereas the toe-off instance estimation was within 70.97 ± 61.55 ms, or $5.78 \pm 5.38\%$ of the gait cycle, for all navigational scenarios tested. The errors in determining the duration of stride time, single support, and double support were within 90.85 ± 68.5 ms ($7.29 \pm 5.27\%$), 77.48 ± 36.30 ms ($6.36 \pm 2.98\%$), and 60.77 ± 24.37 ms ($4.98 \pm 2.09\%$), respectively, for all navigational scenarios. Absolute error in stride duration was acceptable (Pearson correlation coefficient with Vicon's stride duration ranged from $r = 0.53$ to $r = 0.86$). However, absolute errors were too

Table 4

Pearson correlations coefficients (r) and mean of the absolute errors in toe-off instances estimation between Vicon based inspection and the force-moment based algorithm (presented as time difference, in milliseconds, between the instances of initial contact identified on Vicon and the corresponding initial contacts detected by our algorithm, as well as the percentage of this time difference to the corresponding stride time obtained from Vicon)

	Go straight	30° left turn	30° right turn	60° left turn	60° right turn
Right toe	0.9992, 4.1 ± 2.75% (53.54 ± 42.60 ms)	0.9991, 4.57 ± 4.53% (57.61 ± 61.09 ms)	0.9959, 6.26 ± 7.71% (70.67 ± 66.32 ms)	0.9971, 8.22 ± 6.18% (103.56 ± 83.73 ms)	0.9983, 6.05 ± 3.22% (74.65 ± 40.25 ms)
Left toe	0.9985, 5.18 ± 2.75% (66.31 ± 39.29 ms)	0.9984, 5.01 ± 2.49% (62.27 ± 36.01 ms)	0.9962, 6.07 ± 5.85% (65.69 ± 44.94 ms)	0.9976, 7.37 ± 7.14% (95.17 ± 97.96 ms)	0.9987, 5.34 ± 2.52% (66.11 ± 33.55 ms)

Table 5

Pearson correlation coefficients (r) and mean of the absolute errors in stride, double support and left and right single support between Vicon based inspection and the force-moment based algorithm (presented as time difference, in milliseconds, between the instances of initial contact identified on Vicon and the corresponding initial contacts detected by our algorithm, as well as the percentage of this time difference to the corresponding stride time obtained from Vicon)

	Stride	Double support	Right single support	Left single support
Go straight	0.8568, 5.86 ± 2.49% (73.19 ± 34.58 ms)	0.1712[*], 4.34 ± 2.10% (54.56 ± 24.65 ms)	0.3995, 5.24 ± 2.29% (66.52 ± 29.53 ms)	0.4171, 5.38 ± 2.31% (67.23 ± 30.01 ms)
30° left turn	0.7794, 7.50 ± 6.70% (91.79 ± 82.40 ms)	0.1823[*], 5.92 ± 2.32% (70.28 ± 24.23 ms)	0.3524, 6.58 ± 2.81% (79.98 ± 33.17 ms)	0.3134, 7.08 ± 2.97% (86.01 ± 38.91 ms)
30° right turn	0.5286, 6.21 ± 5.21% (73.36 ± 57.21 ms)	0.2620, 5.63 ± 2.08% (67.12 ± 22.72 ms)	0.4663, 5.68 ± 2.84% (66.56 ± 30.73 ms)	0.4323, 6.13 ± 2.83% (72.21 ± 28.06 ms)
60° left turn	0.7812, 8.34 ± 5.98% (106.48 ± 83.00 ms)	0.2215, 4.95 ± 2.06% (62.56 ± 27.69 ms)	0.3329, 6.27 ± 2.73% (79.65 ± 35.27 ms)	0.3354, 6.67 ± 3.29% (82.60 ± 41.79 ms)
60° right turn	0.8076, 8.26 ± 5.04% (110.61 ± 69.43 ms)	0.3431, 4.85 ± 1.95% (60.44 ± 23.36 ms)	0.5302, 6.94 ± 3.11% (85.66 ± 35.89 ms)	0.4507, 6.99 ± 3.37% (86.35 ± 41.11 ms)

[*] Not statistically significant ($p > 0.05$).

high to estimate the single and double support phases with acceptable accuracy. This is due to the fact that double and single support phases are short, approximately 10% of the gait cycle for the double support, which makes the duration of these phases more sensitive to errors in the detection of the heel initial contact instance or the toe-off instance on the opposite foot. Unlike the percentage error reported, the absolute errors in milliseconds were not normalized by the gait cycle time. The errors presented above are based solely on the determination of the heel initial contact and toe-off times from visual inspection of the Vicon's motion capture data by a human observer. These reference instances themselves are prone to errors comparable to the duration of the double support time, 5–10% of the gait cycle [19]. It is clear from the error tables that the error of heel initial contact detection, toe-off time estimation, and the computed stride time, as well as the times of the single and double support phases, generally tend to increase when the walker's user changes direction. This is expected since the forces and moments exerted on the walker's handles include a component reflecting the user's desire to change the direction of the walker, in addition to a component reflecting the user's increased need for support while performing a turn (see Ref. [2]).

Nevertheless, if we limit gait characterization to data collected during straight line segments (through tracking the orientation of the steering wheel using an encoder), we can reduce the errors, and standard deviation of the errors in particular, appreciably. In the case of walking in a straight line, the temporal error in detecting the instances of heel initial contacts were within 67.26 ± 50.38 ms, which is equivalent to $5.27 \pm 3.66\%$ of the overall stride time obtained from Vicon, whereas the toe-off instance estimation were within 66.31 ± 39.29 ms, or $5.18 \pm 2.75\%$ of the gait cycle. The errors in determining the duration of stride time, single support, and double support were within 73.19 ± 34.58 ms $(5.86 \pm 2.49\%)$, 66.52 ± 29.53 ms $(5.24 \pm 2.29\%)$, and 54.56 ± 24.65 ms $(4.34 \pm 2.13\%)$, respectively. The stride time estimated using the method presented here correlated well with stride time computations based on visual inspection of Vicon's data, Pearson correlation coefficient $r = 0.86$ for straight line segments.

The accuracy of our results is comparable to that obtained by Karcnik [19]. In the above mentioned study a simple, fast and straightforward method was developed to automatically derive foot-floor contact information from tracking motion analysis system markers attached to the shoes of the subjects. The system required an accurate calibration of the motion analysis system. However, the method does not obviate the need for the motion capture data [19].

4.2. Limitations

The 60% rule of the gait for toe-off estimation is applicable to normal gait of able bodied subjects on level grounds. However, for patient populations with abnormal gait pathologies, or for inclined ramps, this value may not be applicable. On the other hand, the peak detection algorithm presented here is not suited for on-line procession. Hence, the peak detection algorithm needs further modifications to suit on-line processing.

Similarly, the non-causal digital filter used, as described in Section 3, is suitable for off-line processing. Nonetheless, on-line gait characterization, necessitates substituting the bidirectional filter with a causal filter with minimal phase shift or at least linear phase response with the minimal order necessary to guarantee the on-line processing speed. FIR filters have the linear phase shift characteristics, but FIR filters have an order four times that of the corresponding IIR filter with the same complexity [20]. Meanwhile, the Butterworth IIR filter has minimal phase shift over the filter's band pass when compared to other conventional filters [21]. When designed properly, the magnitude response of the filter is flat and the phase response is approximately linear in the pass-band. With these characteristics and lower order than the corresponding FIR filter, a high order Butterworth filter can be implemented.

5. Conclusion and future work

We can detect heel initial contacts of left and right foot from forces-moments exerted on walker handles with 97% sensitivity and 98% specificity (with a narrow 95% confidence interval of $\pm 1\%$) compared to a human rater inspecting heel initial contact data of the Vicon motion capture system. Based on heel initial contact detection, and toe-off time estimation, we could identify and estimate the duration of strides with acceptable accuracy, less than 6% of the overall stride time, especially when the subjects walked in a straight line. The significance is the potential ability to assess gait characteristics passively outside the lab. Additional sensors on the walker, such as incremental wheel encoders, would allow the derivation of other gait characteristics, such step and stride lengths, as well as average walking velocity. Consequently, the instrumented walker can be used to assist in clinical gait analysis. Since the walker is small and portable, it may allow certain gait analyses to be done longitudinally "in the field", both in the home and out in the community.

A new peak detection algorithm is currently under development; the algorithm uses step lengths history (computed from previous heel initial contacts instances) to adapt the width of the window for each subject and for each estimated initial contact times. A similar data history based approach will be adopted to adapt the toe-off estimation and detection methods. The history-based peak detection and toe-off estimation algorithms may allow the adaptation of the method to cater for abnormal gait pathologies and locomotion disabilities and will hence require validation on a different subject population. We also intend to explore the minimum phase shift Butterworth IIR filtering for the on-line gait characterization method. The enhanced future heel initial contact detection and toe-off detection/estimation algorithms will be validated against methods that would allow the detection of

heel initial contact and toe-off more accurately; such methods may involve the use of heel/toe switches or pressure-sensitive insole inserts in the future. These issues and enhancements will be taken into consideration in future studies that will be conducted with subject populations exhibiting gait anomalies.

Acknowledgement

References

[1] Fay BT, Boninger ML. The science behind mobility devices for individuals with multiple sclerosis. Med Eng Phys 2002;24:375–83.

[2] National Center for Health Statistics. Number of persons using assistive technology by age of person and type of device; 1994, http://www.cdc.gov/nchs/about/major/nhis_dis/ad292tb1.htm.

[3] Wasson G, Sheth P, Alwan M, Granata K, Ledoux A, Huang C. User intent in a shared control framework for pedestrian mobility aids. IROS 2003;3:2962–7.

[4] Fast A, Wang FS, Aderzin RS, Cordaro MA, Ramis J, Sosner J. The instrumented walker: usage patterns and forces. Arch Phys Med Rehabil 1995;76950:484–91.

[5] Bachschmidt RA, Harris GF, Simoneau GG. Walker-assisted gait in reahbilitation: a study of biomechanics and instrumentation. IEEE Trans Neural Syst Rehabil Eng 2001;9(1):96–105.

[6] Chen LC, Chen HC, Wong MK, Tang FT, Chen RS. Temporal stride and force analysis of cane-assisted gait in people with hemiplegic stroke. Arch Phys Med Rehabil 2001;82:43–8.

[7] Aminian K, Rezakhanlou K, De Andres E, Fritsch C, Leyvraz PF, Robert P. Temporal feature estimation during walking using miniature accelerometers: an analysis of gait improvement after hip arthroplasty. Med Biol Eng Comput 1999;37(6):686–91.

[8] Mansfield A, Lyons GM. The use of accelerometry to detect heel contact events for use as a sensor in FES assisted walking. Med Eng Phys 2003;25:879–85.

[9] Pappas IP, Keller T, Mangold S, Popovic MR, Dietz V, Morari M. A reliable gyroscope-based gait-phase detection sensor embedded in a shoe insole. IEEE Sens J 2004;4(2):228–74.

[10] Pappas IP, Popovic MR, Keller T, Dietz V, Morari M. A reliable gait phase detection system. IEEE Trans Rehabil Eng 2001;9:113–25.

[11] Skelly MM, Chizeck HJ. Real-time gait event detection for paraplegic FES walking. IEEE Trans Neural Syst Rehabil Eng 2001;9(1):59–68.

[12] Wasson G, Gunderson J, Graves S, Felder R. An assistive robotic agent for pedestrian mobility. In: International conference on autonomous agents. 2001. p. 169–73.

[13] Wasson G, Gunderson J, Graves S, Felder R. Effective shared control in cooperative mobility aids. FLAIRS 2001:509–13.

[14] Sheldon RS. Quantification of human motion: gait analysis—benefits and limitations to its application to clinical problems. J Biomech 2004;37:1869–80.

[15] Vicon612 Technical Specifications, http://www.vicon.com.

[16] Signal Processing Toolbox User's Guide, The Mathworks Inc.

[17] Alwan M, Wasson G, Sheth P, Ledoux A, Huang C. Passive derivation of basic walker-assisted gait characteristics from measured forces and moments. In: Proceedings of IEEE's 2004 Engineering in Medicine and Biology Conference (EMBC'04). 2004.

[18] Inman VT, Ralston H, Todd F. Human walking. Baltimore: Williams and Wilkins; 1981. p. 26.

[19] Karcnik T. Using motion analysis data for foot-floor contact detection. Med Biol Eng Comput 2003;41:509–12.

[20] Proakis JG, Manolakis DG. Digital signal processing principles, algorithms and applications. Prentice-Hall; 1996.

[21] Samir VG, Joseph AN. Noronha, DESIGN OF IIR FILTERS, http://www.ee.vt.edu/~jnoronha/dsp_proj2_report.pdf.